

Morphology of Condon Domains Phase in Plate-Like Sample

Nathan Logoboy^{1,2,*} and Walter Joss^{1,3}

¹*Grenoble High Magnetic Field Laboratory, MPI-FKF and CNRS P.O. 166X, F-38042 Grenoble Cedex 9, France*

²*The Racah Institute of Physics, The Hebrew University of Jerusalem, 91904 Jerusalem, Israel*

³*Université Joseph Fourier, B.P. 53, F-38041 Grenoble Cedex 9, France*

(Dated: November 30, 2018)

Based on Shoenberg assumption of magnetic flux density dependence of diamagnetic moments which accounts for an instability of strongly correlated electron gas at the conditions of dHvA effect and diamagnetic phase transition (DPT) to non-uniform phase, we investigate the morphology of the Condon domains (CD) in plate-like sample theoretically. At one period of dHvA oscillations the intrinsic structure of inhomogeneous diamagnetic phase (IDP) is governed by the first order phase transitions between different non-uniform phases similar to the high-anisotropy magnetic systems of spin origin, and strongly affected by temperature, magnetic field and impurity of the sample due to the electron correlations. The phase diagrams of evolution of IDP with temperature and small-scale magnetic field in every period of dHvA oscillations are calculated.

PACS numbers: 75.20.En; 75.60.Ch; 75.30.Kz; 71.10.Ca; 71.70.Di; 75.47.Np; 75.40-s; 75.40.Cx; 76.30.Pk; 05.70.Fh

Keywords: A. Strongly correlated electrons; D. Condon domains; D. Diamagnetic phase transition; D. dHvA effect

I. INTRODUCTION

Strongly correlated electron systems are subject of constant interest of physical community. The instability of an electron gas due to strong electron correlations at the conditions of dHvA effect resulting in diamagnetic phase transition (DPT) into inhomogeneous diamagnetic phase (IDP) with formation of Condon domains (CDs) [1], [2] is intensively studied both theoretically and experimentally [3]-[13]. The realization of intrinsic structure of IDP is governed by the competition between long-range dipole-dipole interaction and short-range interaction related to the positive interface energy with typical magnetic length of Larmor radius r_c [1], [14].

There are striking similarities between IDP in normal metals and other strongly correlated systems which undergo phase transition on temperature and magnetic field with formation of complex macroscopic patterns, e. g. the type-I superconductors and thin magnetic films with quality factor exceeding unity. The different technics, including the powder pattern and magneto-optic methods, successfully used for observation of intermediate state of type-I superconductors revealed a very rich structure [15] which in spite of all its complexity, amazingly reminds the variety of domain structures in thin film [18]. The list of the phenomena can be further continued by including other strongly correlated systems which driven by the corresponding parameters exhibit the analogous many-pattern behavior, e. g. Quantum Hall effect system, showing the charge density wave instability with formation of stripe and bubble phases [19], spin-glasses [20], itinerant metamagnets [21]-[23], the Saffman-Taylor

instability of fluid-ferrofluid interface in rotating Hele-Shaw cells [24] and Langmuir monolayers [25]. At the background of these phenomena, the model of simple lamina periodic domain structure (PDS) of normal metals [27]-[29] associated with CDs and used for explanation of electron instability seems to be rather simplified. Indeed, the new experiments on observation of diamagnetic domains by use of a set of Hall probes at the surface of the plate-like sample of silver [3] reveal rather complicated domain structure which only at certain conditions, with tilting the sample relative to applied field, transforms into regular laminar structure similar to the observation of intermediate state of type-I superconductor [30]. Muon spin rotation spectroscopy (μ SR) being a powerful method for investigation of complex materials was successfully used for studying CDs [6]-[9]. The series of excellent experiments on investigation of diamagnetic instability by methods of μ SR spectroscopy [6]-[9] prove the existence of CD phase in beryllium, white tin, aluminum, lead and indium, but reveal also contradictions in attempts of quantitative analysis in the framework of existent theoretical considerations.

The specific case of evolution of domain structure for two-dimensional electron gas in ultra-thin magnetic films with finite thickness $L \lesssim r_c$ was considered in [28]. It was shown that the electron system undergoes the phase transition into a domain state which can cross over into a modulated, or vortex, state with decreasing of the sample thickness. The consideration was restricted by the center of the period of dHvA oscillations. While it is known that IDP occupies only a part of dHvA period, it would be extremely interesting to investigate the morphology of the domain patterns with the change of the magnetic field within one dHvA period. The influence of magnetic field on PDS at the conditions of diamagnetic instability was investigated in [29] where the dependencies of the period of domain structure on magnetic field and film thick-

*Electronic address: logoboy@phys.huji.ac.il

ness were calculated numerically. In particular, it was demonstrated by numerical calculations that the width of the domains with favorable direction of magnetization increases and the width of the domains with unfavorable direction of magnetization decreases with field goes away from the center of dHvA period. The transformation of PDS into modulated state near the critical point $a = 1$ at the center of dHvA period was also illustrated. Unfortunately, the critical fields corresponding to transitions between different domain structures within dHvA period, including bubble lattice, separated bubbles and so on were not calculated and the phase diagrams were not constructed.

In [13] the equilibrium set for the system of strongly correlated electron gas at the conditions of dHvA effect was investigated in the framework of catastrophe theory. It was shown that in every period of dHvA oscillations the discontinuities of order parameter accompanied DPT is handled by Riemann-Hugoniot catastrophe implying the standard scenario for DPT, e.g. DPT is of the second order at the center of dHvA period, weakly first order in the nearest vicinity of this point and is of the first order at the rest part of the dHvA period. Thus, similar to other magnetic systems, e. g. the spin [18] and metamagnetic ones [23], the DPT can be realized in rich background of nonuniform phases depending on the shape of the sample. The studies of diamagnetic instability [13] are based on postulates of the phase theory when the irreversibility effects are ignored, and the results are applied for ellipsoidal uniformly magnetized phases in uniform external magnetic field. Thus, the shape effect accounted for by use of the conception of demagnetizing coefficient n consists in expansion of the magnetic field range for IDP existence $|x| \leq x_c(n)$ with increase of n .

The calculations based on bifurcation theory allows to eliminate all possible stable equilibria of the strongly correlated electron system, but the conclusion about realization of non-uniform states and evolution of IDP can be done only on the basis of consideration of global minimum of the free energy of a system for given configuration of domain patterns, including the energy of long-range dipole-dipole interaction, the energy of the interphase boundaries and the magnetic energy in applied field. The calculations become a rather complicated problem due to existence of non-local dipole-dipole interaction which can not be accounted for by use of demagnetizing coefficient contrary to the studies performed in the framework of phase theory. Although, the relevant problems were solved in the physics of magnetism of spin origin [18], the general picture of formation of non-uniform phases is complicated by the electron correlations due to non-local magnetic interaction between electrons [27].

Using the methods developed in the physics of magnetic materials, for a plate-like sample we calculate the phase diagrams related to complicated intrinsic structure of IDP which can realized through the formation of variety of different domain patterns, including modulated states in the nearest vicinity of critical point and regular

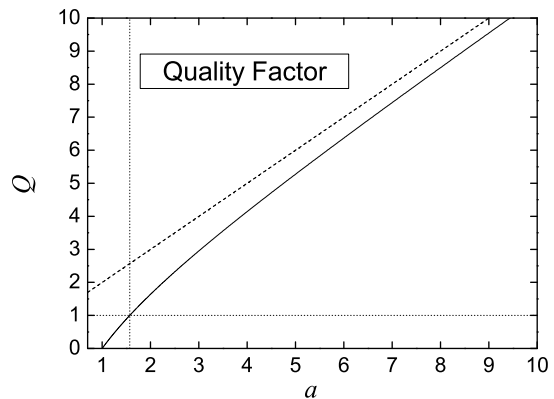


FIG. 1: Quality factor Q Eq. (4) defined for the plate-like sample of normal metal at the conditions of strong dHvA effect is plotted as a function of reduced amplitude of dHvA oscillations a (solid line). For $a \geq \pi/2$ the macrostructure of domain patterns are expected to be similar to the domain structure of thin high-anisotropy magnetic films of spin origin due to $Q \geq 1$. The dash line is asymptote of function $Q = Q(a) \rightarrow a + 1$ for $a \rightarrow +\infty$.

parallel band domains which transferred into separated band domains, close-packed bubble lattices and isolated bubbles with changing the small-scale magnetic field x within one period of dHvA oscillations. We show that evolution of domain structure with temperature is different at the center of the period of dHvA oscillations and its other part within the range of existence of IDP.

The paper is organized as follows. In Sec. II, we introduce the model and relevant results of catastrophe theory which at proper choice of control variables provides a convenient tool for investigation of DPT. In Sec. III we present and discuss the general conditions for realization of the DPT in the sample with taking into account the long-range dipole-dipole interaction and calculate the critical fields which characterized the non-uniform phases. We show that convectional scenario of transformation of magnetic phases is influenced by electron correlations resulting in strong temperature and magnetic field dependency of critical fields. Finally, in Sec. IV, we summarize our main conclusions.

II. MODEL

The properties of strongly correlated electron system at the conditions of dHvA effect in one harmonic approximation are described by the free energy functional

$$G(y; a, x) = G^{(unif)} + G^{(grad)}, \quad (1)$$

where

$$G^{(unif)} = a \cos(x + y) + \frac{1}{2}y^2, \quad (2)$$

$$G^{(grad)} = \frac{1}{2}ar_c^2(\partial_\zeta y)^2.$$

Here, the small-scale magnetic field $x = k\mu_0(H - H_a)$ is the increment of the large-scale internal magnetic field $\mu_0 H$ and external (applied) magnetic field $\mu_0 H_a$, y is oscillating part of reduced magnetization, $k = 2\pi F/(\mu_0 H_a)^2 = 2\pi/\Delta H$, F is the fundamental frequency of the dHvA oscillations corresponding to the extreme cross-section of Fermi surface, ΔH is dHvA period and $a = \mu_0 \max\{\partial M/\partial B\}$ is differential magnetic susceptibility [27]. In physical units x is of the order of ~ 1 -10 mT depending on the properties of the electron system, while $\mu_0 H$ is ~ 1 -10 T. The gradient term in Eq. (2) accounts for the short-range correlations on the scale of r_c [14], ζ is coordinate.

In the framework of bifurcation theory the diamagnetic instability can be handled by cusp catastrophe [13]. In case of thin film one can show that the bifurcation set in the $a - x$ plane of control variables a and x is described by the following expression (see Appendix for details)

$$a \cos(\sqrt{a^2 - 1} - |x_c - y(a, x_c)|) = 1, \quad (3)$$

where the magnetization $y = y(a, x_c)$ is given explicitly by $y = a \sin(x_c + y)$. Eq. (3) defines the function $a = a(x_c)$ which is plotted in Fig. 4(a). The bifurcation curve $a = a(x_c)$ divides the $a - x$ plane onto two parts, the inner part is occupied by IDP, while the outer one corresponds to uniform state. Offering a systematic way to study the diamagnetic instability, the catastrophe theory implies the different scenario of formation and evolution of domain patterns at the center of the period of dHvA oscillations and away of it. At the center of dHvA period, the stability criterion for CD formation is $a \geq 1$ and theory predict the second order phase transition. The crossing of bifurcation set with lowering of temperature results in appearance of two-fold degenerate equilibria, thus, one would expect the stratification of the sample into the domains of equal widths and appearance of PDS due to the essential decrease in magnetostatic energy. The steady-state domain size is defined by competition between long-range dipole-dipole interaction and short-range electron interaction on the scale of r_c and calculated by standard method based on minimization of total energy containing two terms, e. g. dipole-dipole energy and surface energy of separation of two domains [18]. Away of the center of dHvA period the transition is of the first order and takes place at lower temperature. At this condition the crossing of bifurcation set leads to appearance of additional local minimum in free energy. The energy corresponding to this new minimum is higher than the energy of the previous state. But, even in this case the formation of non-uniform phase can decrease the net energy due to decrease of magnetostatic energy. Thus, at the vicinity of phase boundary a probable new non-uniform phase consists of fully occupied areas with equal magnetization and depletion regions with different magnetization, e.g. separate bubbles embedded into uniformly magnetized sample. With further decrease of temperature the energy difference between two local minima in free energy decreases, and further decrease of net en-

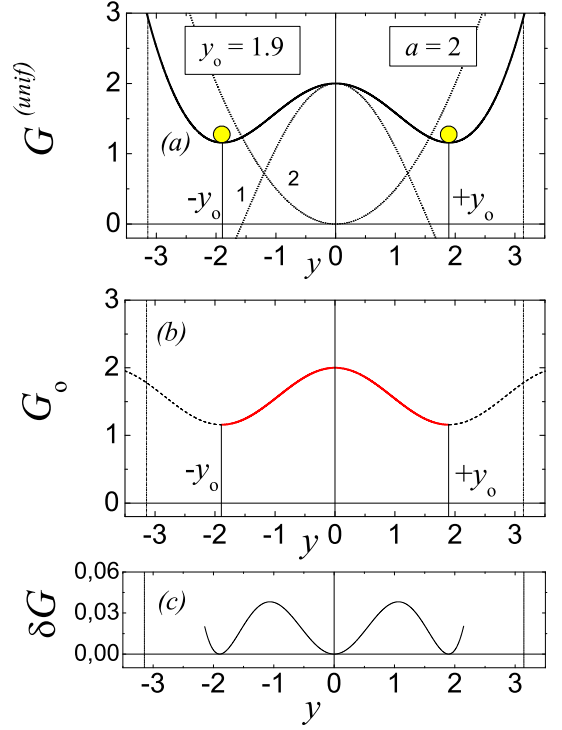


FIG. 2: (color online) Shown are (a) the free energy density $G^{(unif)}$ (solid line) as a function of magnetization y with two contributions (curves 1 and 2) according to Eq. (2); (b) the approximated free energy density G_0 Eq. (8) at the relevant range $y \leq |y_0|$ where $\pm y_0 = \pm 1.9$ are two minima and (c) the free energy difference $\delta G = G^{(unif)} - G_0$. The accuracy of the approximation $G^{(unif)} \approx G_0$ is $\sim 10^{-2}$. The calculations are made at the center of the period of dHvA oscillations with the value of differential magnetic susceptibility $a = 2$.

ergy can be achieved by organizing the separated bubbles into bubbled lattice and formation PDS of band domains with volume fraction linear dependent on magnetic field.

In Sec. III we show that in plate-like sample the IDP has complicated intrinsic structure and calculate the phase diagrams corresponding to evolution of IDP within the period of dHvA oscillations.

III. RESULTS AND DISCUSSIONS

Before proceeding with calculation we define the quality factor for a plate-like sample according to

$$Q = \frac{\partial_{yy}^2 G^{(unif)}}{\partial_{yy}^2 G^{(d-d)}} \bigg|_{y=y_0} = 1 - a \cos y_0, \quad (4)$$

where $G^{(d-d)} = y_0^2/2$ is demagnetizing energy for uniformly magnetized plate-like sample. Here, $y_0 = y_0(a)$ is the magnetization of two-fold degenerate uniform ground state given explicitly by the equation

$$y_0 - a \sin y_0 = 0 \quad (5)$$

at $a \geq 1$. The function $Q = Q(a)$ is plotted in Fig. 1 which shows that $Q \geq 1$ for all values of $a \geq \pi/2$. Differential magnetic susceptibility $a = a(\mu_0 H, T, T_D)$ is a function of magnetic field $\mu_0 H$, temperature T and Dingle temperature T_D . Therefore, it follows from Fig. 1 that in a wide range of temperature and magnetic field corresponding to the diamagnetic instability, the magnetic properties of strongly correlated electron gas at the conditions of the diamagnetic instability are expected to be analogous to the conventional high-anisotropic magnetic materials which are characterized by quality factor $Q > 1$.

Variation of the free energy G Eq. (1) with respect to the magnetization y at the center of dHvA period leads to the following differential equation

$$a \sin y - y + ar_c^2 \partial_{\zeta\zeta}^2 y = 0 \quad (6)$$

The first integral of Eq. (6)

$$ar_c^2 (\partial_{\zeta} y)^2 = 2a \cos y + y^2 + C, \quad (7)$$

forms the basis for investigation of non-uniform phases in one-dimensional problems. By choosing a different integration constant C one can obtain the solutions describing separate domain walls, PDS and modulated structures. The corresponding problems in physics of magnetic materials were solved long ago (see, [18]). We find it useful to present the analytical solutions of Eq. (6) related to PDS for the system exhibiting the diamagnetic instability, the first, to see the close analogy with the physics of magnetic phenomena of spin origin and, the second, the periodic analytical solutions for IDP were not reported as far as we aware of.

In a limit $a - 1 \rightarrow 0^+$, one can use expansion of RHS of Eq. (6) in powers of b due to $b \leq b_0 = \sqrt{6(a-1)} \ll 1$. Thus, Eq. (6) can be integrated resulting in periodic distribution of magnetic induction $b = b_0 \operatorname{sn}(\zeta/\delta_1, k)$ with a period $D = 4K(k)\delta_1$, where sn is Jacobi elliptic function, K is complete elliptic integral and k is elliptic modulus. The parameter $\delta_1 = r_c \sqrt{(1+k^2)/(a-1)}$ is the domain wall width. At $k=1$, $K \rightarrow \infty$ we arrive to the solution $b = b_0 \tanh(\zeta/\delta_1)$ describing the separate domain wall [28]. At $k=0$, we obtain the modulated structure $b = A \sin(q_0 \zeta)$ [28], where $A = \sqrt{6(a-1)}$ and $q_0 = r_c^{-1} \sqrt{a-1}$ are the amplitude and wave vector.

In case of $a - 1 \gtrsim 1$, one can see that the main contribution is due to the first term in $G^{(unif)}$. In this case the quality factor $Q > 1$ (see, Fig. 1), the sample is characterized by high anisotropy, and at the relevant range $y \leq |y_0|$ with a great accuracy the potential $G^{(unif)}$ can be approximated by trigonometric function (Fig. 2) corresponding to two-fold degenerate equilibria $y = \pm y_0$

$$G^{(unif)} \approx G_0 = -\frac{1}{2} K_0 \sin^2 \left(\frac{\pi}{2} \frac{y}{y_0} \right), \quad (8)$$

where

$$K_0 = 4a \sin^2 \frac{y_0}{2} (1 - a \cos^2 \frac{y_0}{2}) > 0 \quad (9)$$

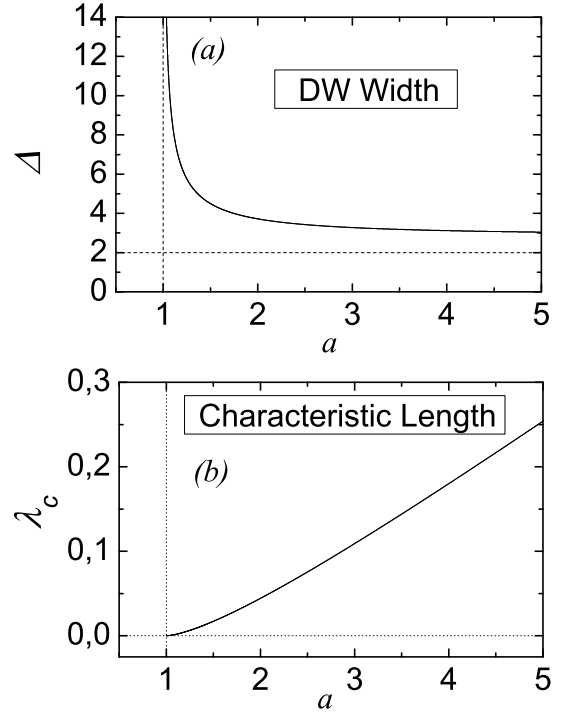


FIG. 3: (a) Domain wall width Δ and (b) characteristic length λ_c are plotted as functions of reduced amplitude of dHvA oscillations a . The dash lines in (a) show the asymptotes. In calculations of λ_c (b) the value of $r_c/L = 10^{-2}$ was used.

is a function of a and y_0 and analogous to the constant of easy-axis crystallographic anisotropy in physics of magnetic materials. In Eq. (8) we omitted the unessential constant. Introducing a new variable $\Theta = \pi y/2y_0$, we rewrite Eq. (1) in a form

$$G = -\frac{1}{2} K_0 \sin^2 \Theta + \frac{1}{2} A (\partial_{\zeta} \Theta)^2, \quad (10)$$

with account of Eq. (8). The parameter $A = a(2r_c y_0/\pi)^2$ characterizing the the short-range interaction is analogous to the exchange constant for spin systems. This confirms the close analogy between high-anisotropy ferromagnetic and the system exhibiting the diamagnetic instability. Minimization of free energy density Eq. (10) allows to obtain the non-uniform state described by periodic function

$$y = \frac{2y_0}{\pi} \sin^{-1} [\operatorname{sn}(\frac{\zeta}{\delta_2}, k)], \quad (11)$$

where $\delta_2 = k\sqrt{A/K_0}$. If a much greater than 1, then it is follows from Eq. (5) that $y_0 \approx \pi$, the parabolic term in Eq. (2) is negligible, and the solution has a simple form $y = 2 \sin^{-1} \operatorname{sn}(\zeta/\delta_2, k)$ with $\delta_2 = r_c k$. At $k=1$, $K \rightarrow \infty$ we arrive to the solution $y = 2 \sin^{-1} \tanh(\zeta/\delta_2)$ analogous to separate 180° Bloch domain wall.

Similar to the high-anisotropy magnetic films in perpendicular magnetic field a variety of different domain

patterns can form in a thin film of normal metal at the condition of diamagnetic instability $a \geq a_c$ where a_c depends on small-scale magnetic field x and is defined explicitly by Eq. (3). Following [16], [17] and [18] we calculated the phase diagrams in the $a - x$ plane describing the intrinsic properties of IDP at one period of dHvA oscillations. In calculations we neglect the structure of the domain walls assuming that the size of the domain is large compared to the domain wall width, thus, characterizing the domain wall by specific wall energy

$$\sigma = \frac{4r_c}{\pi} a^{1/2} y_0 [Q^2 - (a-1)^2]^{1/2} \quad (12)$$

and dimensionless domain wall width

$$\Delta = \frac{\delta}{r_c} = \frac{4}{\pi} \frac{a^{1/2} y_0}{[Q^2 - (a-1)^2]^{1/2}}. \quad (13)$$

We introduce also the commonly used in phase diagram calculations [18] dimensionless characteristic length

$$\lambda_c = \frac{\sigma}{2L}, \quad (14)$$

where L is the width of the plate. The quantities $\sigma = \sigma(a)$ Eq. (12), $\Delta = \Delta(a)$ Eq. (13) and $\lambda_c = \lambda_c(a)$ Eq. (14) are characterized by strong dependencies on temperature, magnetic field and purity of the sample through the differential magnetic susceptibility a (Fig. (3)). At the vicinity of point $a = 1$, the behavior of Δ and λ_c signalizes about the presence of critical point of the system. Near the critical point, $a \rightarrow 1+0^+$, the spontaneous fluctuations become large, the length scale of fluctuations $\xi \sim \delta \sim (a-1)^{-1/2}$ has a power law of divergence, and the characteristic length $\lambda_c \sim \sigma \sim (a-1)^{3/2} \rightarrow 0$. There is no typical scale length except of the trivial lower (atomic distance) and upper macroscopic (the size of the system L) size scales.

The standard procedure of calculation of phase diagrams consists in consideration of different configurations of domain patterns and minimization of free energy density containing three terms, e. g. dipole-dipole energy, the surface energy of the boundary states and the energy of interaction with external magnetic field (Zeeman term) [18]. In connection to this, there are two main mutually related to each other features that make the calculations for strongly correlated electron gas at the conditions of diamagnetic instability different from analogous calculations in physics of magnetic materials. The first, the magnetic moments of oppositely magnetized uniform phases differ on values. And, the second, the energy of interaction of magnetization with magnetic field is not trivial, it is included explicitly in the first term of Eq. (2) and defines the magnetic field dependence of diamagnetic moments $y_{\pm} = y_{\pm}(x)$ of uniformly magnetized phases within the period of dHvA oscillations due to

$$y = -\partial_x G^{(unif)} = a \sin(x + y). \quad (15)$$

We demonstrate these differences by consideration of isolated band domains. Imbedding a uniformly magnetized

band of width W and of magnetization $y_- - y_+$ into a plate of thickness L and opposite magnetization y_+ , we can write the total energy

$$e^{(tot)} = \frac{g(w)}{2\pi} (\mu_+ + \mu_-)^2 - \mu_+ (\mu_+ + \mu_-) w + \lambda_c, \quad (16)$$

where the function

$$g(w) = 2w \tan^{-1} w + \frac{1}{2} \ln[w^{-2}(1+w^{-2})^{w^2-1}]. \quad (17)$$

is defined in [18] in slightly different form, $w = W/L$ is reduced band width and $\mu_{\pm} = y_{\pm}(\pm x)$. In derivation of Eq. (16) we used $y_-(x) = -y_+(-x)$ (see, also Fig. 4(b)). The first term in Eq. (16) is the self-energy of imbedded band, the second term describes the interaction of the band with uniformly magnetized matrix [18] and the third term corresponds to interface boundary energy. Minimization of total energy of isolated band with respect to w results in

$$\frac{2\pi\mu_+}{\mu_+ + \mu_-} = \partial_w g, \quad (18)$$

which defines the equilibrium band width $w = w(x, a)$ as a function of magnetic field x and differential magnetic

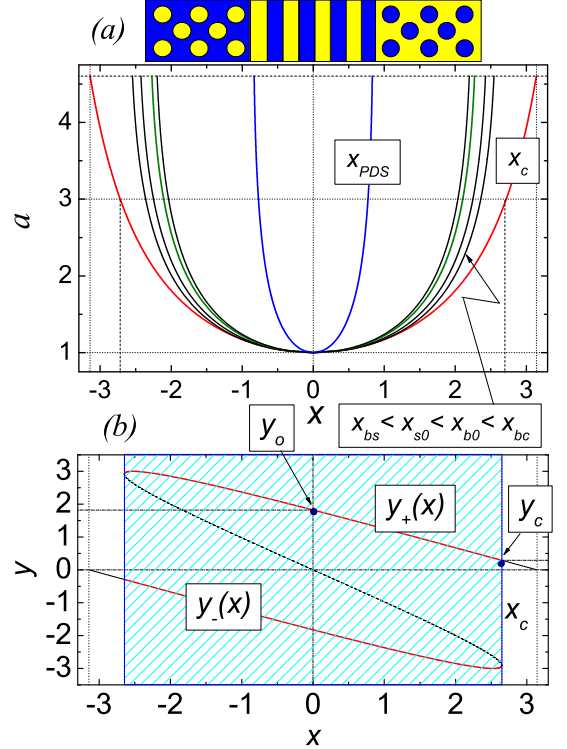


FIG. 4: (color online) (a) Phase diagrams in $a - x$ plane for one period of dHvA oscillations and (b) magnetic field dependencies of the magnetization $y_{\pm} = y_{\pm}(x)$ (solid lines) calculated in the framework of phase theory for $a=3$. The characteristic fields x_{PDS} , x_{bs} , x_{s0} , x_{b0} , x_{bc} and x_c are explained in the text. The sparse area in (b) corresponds to IDP. In calculations of phase diagrams the value of $r_c/L = 10^{-2}$ is used.

susceptibility a . Another equation corresponding to the saturation state is $e^{(tot)} = 0$ [18] which with the help of Eq. (18) gives rise to

$$\frac{4\pi\lambda_c}{(\mu_+ + \mu_-)^2} = w\partial_w g - g. \quad (19)$$

For $a \gtrsim 2$ the function μ_{\pm} can be approximated by linear function $\mu_{\pm} = y_0 \pm (y_0 - y_c)x/x_c$, where $y_c = y(x_c)$ is the value of magnetization at the bifurcation set (see, Fig. 4(b)). In this case, instead of Eqs (18) and (19) we obtain

$$\begin{cases} 1 - x/\tilde{x}_c = \pi[2 \tan^{-1} w + w \ln(1 + w^{-2})] \\ 2\pi\lambda_c/y_0^2 = w^2 \ln(1 + w^{-2}) + \ln(1 + w^2), \end{cases} \quad (20)$$

where $\tilde{x}_c = (1 - y_c/y_0)^{-1}x_c \approx x_c$ is a saturation field which in a limit $a \gg 1$ coincides with the critical field x_c defined by bifurcation set (3). Eqs. (20) define a parametric function $a = a(x_{s0})$ with w as a parameter. This function is plotted in Fig. 4 together with the family of phase boundary curves corresponding to other possible pattern configurations, e. g. periodic parallel band structure, bubble lattice and isolated bubbles, calculated in a similar way. We adopted the indexes of characteristic fields [18], e. g. x_{bc} is the bubble collapse field, x_{b0} is the bubble lattice saturation field, x_{s0} is the saturation field for isolated non-interacting bands and x_{bs} is the strip-out characteristic field. The magnetic field x_{PDS} is the characteristic field below which the PDS of parallel bands exists. At the center of dHvA oscillations, $x = 0$, the CDs of equal width exist. With increasing of the small-scale field, x , the volume fraction of up-domains increases in the expense of down-domains. Close to the boundary $x \rightarrow x_{PDS} - 0^+$, the distortions of regular CD phase, e. g. bending, are expected. When $x = x_{PDS} + 0^+$, this structure transforms into the hexagonal bubble lattice which is more favored energetically. The further increase of the field x results in the decrease of the bubble density till the transformation of the lattice into the separated bubbles which exist as a minority phase in the range $x_{bs} < x < x_{bc}$. It follows from our analysis that the existence of different inhomogeneous phases is strongly affected by large-scale magnetic field $\mu_0 H$, temperature T and Dingle temperature T_D due to the corresponding dependencies of the differential magnetic susceptibility $a = a(\mu_0 H, T, T_D)$ which can be used for experimental studies of predicted effects.

IV. CONCLUSIONS

We investigated theoretically the phase characteristics of the IDP caused by the arising instability of strongly correlated electron gas in high magnetic field and low temperature. We show that the formation of IDP can realized through a variety of different diamagnetic phases, including the plane-parallel band structure, isolated non-interacting bands, hexagonal lattice of magnetic bubbles and separated non-interacting bubbles.

The evolution of the domain patterns is different at the center of dHvA period and away of it. While at $x = 0$ the lowering of a temperature results in formation of modulated structure in the nearest vicinity of critical point which with further decrease of temperature transforms into regular CD structure with the domains of equal width, away of the center $x \neq 0$ the system of strongly correlated electron gas can underdo the series of phase transitions with formation of different domain patterns depending on differential magnetic susceptibility a .

We think that the appearance of distinct complex structure of IDT has to affect the transport properties of electron gas under the diamagnetic instability, but this is beyond the scope of the article. The Condon domains provide an excellent system for fundamental research, and we hope that our studies will stimulate the further experiments on observation of electron instability at the conditions of strong dHvA effect and investigation of intrinsic structure of the non-uniform diamagnetic phases.

Acknowledgments

We are indebted to V. Egorov, R. Kramer and I. Sheikin for fruitful discussions.

APPENDIX: CUSP CATASTROPHE

1. Bifurcation Set

Let us introduce a new function

$$\phi(z; \alpha) = z - \frac{\sin z}{1 + \alpha_1} - \alpha_2, \quad (A.1)$$

which is a sufficiently smooth two-parametric function of $(z, \alpha) \in \mathbb{R}^3$, where $\alpha = (\alpha_1, \alpha_2)$ is two-component vector which controls the approach to critical point. The function Eq. (A.1) describes the equilibrium properties of the system of strongly correlated electron gas with magnetic induction $b = z$ as the phase-state variable dependent on two adjustable, or control parameters, e. g. reduced amplitude of dHvA oscillations a and increment of internal magnetic field x , connected to the components of the vector $\alpha = (\alpha_1, \alpha_2)$ by the relations

$$a = (1 + \alpha_1)^{-1}, \quad x = \alpha_2. \quad (A.2)$$

In mean-field theory of critical behavior of system [31], the parameter α_1 controls the amount of ordering, or the value of order parameter (magnetic induction splitting in case of DPT), while parameter α_2 breaks the $Z(2)$ symmetry of order parameter. We assume that the system has an equilibrium $z = z_0$ with eigenvalue $\lambda = \phi_z(z_0; \alpha_0) = 0$ at $\alpha = \alpha_0$, e. g.

$$\begin{cases} \phi(z; \alpha) = 0 \\ \partial_z \phi(z; \alpha) = 0. \end{cases} \quad (A.3)$$

The Jacobian matrix of the system (A.3)

$$\mathbf{J} = \begin{pmatrix} \partial_z \phi & \partial_{\alpha_1} \phi & \partial_{\alpha_2} \phi \\ \partial_{zz} \phi & \partial_{z\alpha_1} \phi & \partial_{z\alpha_2} \phi \end{pmatrix} \quad (\text{A.4})$$

has a maximal rank $r = 2$ at point (z_0, α_0) due to non-zero value of the determinant

$$\det \begin{pmatrix} \partial_{\alpha_1} \phi & \partial_{\alpha_2} \phi \\ \partial_{z\alpha_1} \phi & \partial_{z\alpha_2} \phi \end{pmatrix} = \frac{1}{1 + \alpha_1^0} \neq 0. \quad (\text{A.5})$$

Therefore, the system of Eqs. (A.3) defines a smooth curve L in the joint space \mathbb{R}^3 of phase-state and control variables (z, α) . According to Eqs. (A.3) this curve corresponds to the double degenerated points, passes through the point (z_0, α_0) belonging to the surface of equilibrium states $\phi(z; \alpha) = 0$ and can be parameterized by z due to non-zero value of the determinant Eq. (A.5). Actually, in this case the existence of the two following smooth functions of z

$$\alpha = \alpha(z), \quad (\text{A.6})$$

is provided by the implicit function theorem. For $\phi(z; \alpha)$ defined by Eq. (A.1) one can obtain

$$\begin{cases} \alpha_1 = -2 \sin^2(z/2) \\ \alpha_2 = z - \tan z. \end{cases} \quad (\text{A.7})$$

The standard projection operator map the curve $L \subset \mathbb{R}^3$ onto the space of control variables (α) giving rise to bifurcation set. The straightforward calculation based on eliminating of z in (A.7) allows to obtain the following expression for the function $\alpha_2 = \alpha_2(\alpha_1)$:

$$\alpha_2 = \cos^{-1}(1 + \alpha_1) - \frac{(-\alpha_1)^{1/2}(2 + \alpha_1)^{1/2}}{1 + \alpha_1}. \quad (\text{A.8})$$

The function $\alpha_2 = \alpha_2(\alpha_1)$ Eq. (A.8) defines the bifurcation curve on the plane of control variables (α_1, α_2) where a fold bifurcation occurs. When $\alpha_1, \alpha_2 \ll 1$, Eq. (A.8) can be simplified resulting in standard cusp bifurcation set

$$(2\alpha_1)^3 + (3\alpha_2)^2 = 0, \quad (\text{A.9})$$

which is a semicubic parabola.

From Eq. (A.8) with use of relation (A.2) recalling that for plate-like sample $x = x_c - y$ where x_c is external magnetic field, we arrive to Eq. (3).

In next section for completeness, we present the derivation of the normal form for the system describe by Eq. (A.1). The real use of the normal form consists in scaling the original problem to the other one which is much simpler to solve.

2. Normal Form Derivation

It follows from Eqs. (A.1), (A.3) that there exists the equilibrium point of the system $z = 0$ for which the cusp bifurcation conditions

$$\begin{cases} \partial_z \phi(0; \mathbf{0}) = 0 \\ \partial_{zz} \phi(0; \mathbf{0}) = 0 \end{cases} \quad (\text{A.10})$$

are satisfied. It is important to note that $\partial_{zzz} \phi(0; \mathbf{0}) \neq 0$. Thus, expanding the function $\phi(z; \alpha)$ Eq. (A.1) in a Taylor series with respect to z at $z = 0$ and performing a linear scaling of the phase-state variable z

$$\eta = 6(1 + \alpha_1)z, \quad (\text{A.11})$$

one can arrive to the following normal form for cusp bifurcation

$$f(\eta; \beta) = \beta_1 - \beta_2 \eta + \eta^3, \quad (\text{A.12})$$

where the components of the vector function $\beta = \beta(\alpha)$ are the new control variables defined by the following relations

$$\beta_1 = -6^4 \alpha_2 (1 + \alpha_1)^4, \quad \beta_2 = -6^3 \alpha_1 (1 + \alpha_1)^3. \quad (\text{A.13})$$

The analysis of the normal form Eq. (A.12) which is topologically equivalent to the function Eq. (A.1) is straightforward (see, e. g. [32]). In particular, for $|\alpha_1| \ll 1$ it gives the bifurcation set (A.9) in the vicinity of triple degenerate point.

-
- [1] J. H. Condon, Phys. Rev. 45, (1966) 526.
 - [2] J. H. Condon and R. E. Walstedt, Phys. Rev. Lett. 21, (1968) 612.
 - [3] R. B. G. Kramer, V. S. Egorov, V. A. Gasparov, A. G. M. Jansen, and W. Joss, Phys. Rev. Lett. 95, (2005) 267209.
 - [4] R. B. G. Kramer, V. S. Egorov, A. G. M. Jansen, and W. Joss, Phys. Rev. Lett. 95, (2005) 187204.
 - [5] M. I. Tsindlekht, N. Logoboy, V. S. Egorov,

- R. B. G. Kramer, A. G. M. Jansen, and W. Joss, Phys. of Low Temp. 32, (2006) 1129.
- [6] G. Solt, C. Baines, V. S. Egorov, D. Herlach, E. Krasnoperov and U. Zimmermann, Phys. Rev. Lett. 76, (1996) 2575.
- [7] G. Solt, C. Baines, V. S. Egorov, D. Herlach, and U. Zimmermann, Phys. Rev. 59, (1999) 6834.
- [8] G. Solt and V. S. Egorov, Physica B 318, (2002) 231.
- [9] G. Solt, Solid State Comm. 118, (2001) 231.

- [10] N. Logoboy, A. Gordon, I. D. Vagner, and W. Joss, Solid State Comm. 134, (2005) 497.
- [11] N. Logoboy and W. Joss, Solid State Comm. 139, (2006) 240.
- [12] N. Logoboy and W. Joss, Solid State Comm. 139, (2006) 191.
- [13] N. Logoboy and W. Joss *not published*.
- [14] I. Privorotskii, *Thermodynamic Theory of Domain Structure* (Israel University Press, New York: Wiley and Jerusalem, 1976).
- [15] J. D. Livingstone and W. DeSorbo, in Superconductivity, edited by R. D. Parks (Marcel Dekker, New York 1969).
- [16] C. Kooy and U. Enz, Philips. Res. Repts. 15, (1960) 7.
- [17] J. A. Cape and G. W. Lehman, J. Appl. Phys. 42, (1971) 5732.
- [18] A. Hubert and R. Schäfer, *Magnetic Domains - the Analysis of Magnetic Microstructures* (Springer-Verlag, Heidelberg, 2002).
- [19] A. A. Koulakov, M. M. Fogler, and B. I. Shklovskii, Phys. Rev. Lett. 76, (1996) 499.
- [20] M. Mezard, G. Parisi and M. A. Virasoro, *Spin Glass Theory and Beyond* (World Scientific Publishing Co., Inc., Singapore, 1987).
- [21] H. Yamada, Physica B 391, (2007) 42.
- [22] S. A. Grigera, P. Gegenwart, R. A. Borzi, F. Weickert, A. J. Schofield, R. S. Perry, T. Tayama, T. Sakakibara, Y. Maeno, A. G. Green, and A. P. Mackenzie, Science 306, (2006) 1154.
- [23] B. Binz, H. B. Braun, T. M. Rice, and M. Sigrist, Phys. Rev. Lett. 96, (2006) 196406.
- [24] J. A. Miranda, Phys. Rev. E. 62, (2000) 2985.
- [25] P. Heinig, P. Steffen, S. Wurlitzer, and T. M. Ficher, Langmuir 17, (2001) 6633.
- [26] I. M. Lifshitz and A. M. Kosevich, Sov. Phys. JETP 2, (1956) 636.
- [27] D. Shoenberg, *Magnetic Oscillations in Metals* (Cambridge University Press, Cambridge, England, 1984).
- [28] R. S. Markiewicz, Phys. Rev. B. 34, (1986) 4172.
- [29] M. A. Itskovsky, G. F. Kventsels, and T. Maniv, Phys. Rev. B. 50, (1994) 6779.
- [30] Yu. V. Sharvin, Zh. Eksp. Teor. Fiz. 33, (1957) 1341 [Sov. Phys. JETP 6, (1958) 1031].
- [31] L. P. Kadanoff, *Statistical Physics: Static, Dynamics and Renormalization* (World Scietific, Singapore, New-York, London, Hong Kong, 2000).
- [32] Y. A. Kuznetsov, *Elements of Applied Bifucation Theory* (Springer-Verlag, New-York, Berlin, Heidelberg, 1998).